

# Spatial characteristic of carbon emission intensity under "dual carbon" targets: Evidence from China

Gang Zeng<sup>1,\*</sup>, Yi Guo<sup>1</sup>, Song Nie<sup>3</sup>, Keyan Liu<sup>2</sup>, Yue Cao<sup>2</sup>, Ling Chen<sup>1</sup>, Dezhe Ren<sup>1</sup>, Jiaqi Zhang<sup>1</sup>, Bowen Yan<sup>2</sup>

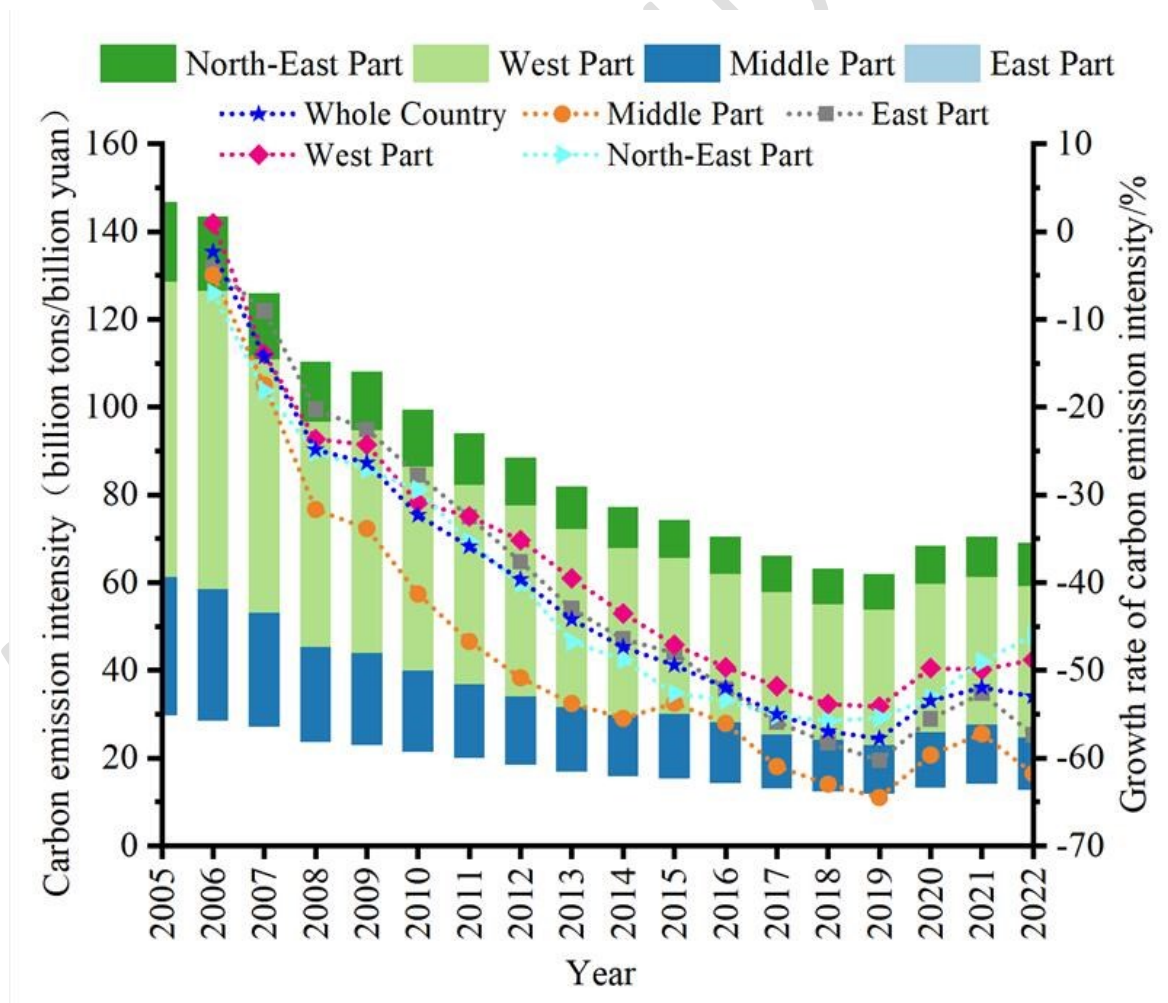
1.School of Economics and Management, Civil Aviation University of China, Tianjin, 300300, China

2.School of Transportation Science and Engineering, Civil Aviation University of China, Tianjin, 300300, China

3. School of Economics, Nankai University, Tianjin, 300071, China

Corresponding author\*: gzeng666@foxmail.com

## Graphical Abstract



**Abstract:** Reducing carbon emissions is one of the important ways to achieve the goal of "dual carbon". Taking carbon emission intensity as the research object, this paper analyzes the spatial effects of carbon emission intensity at

---

provincial level in China during 2005-2022 by Kaya extended model, standard deviation ellipse, Theil index and kernel density analysis model. The results show that: (1) Overall, the distribution of carbon emission intensity in China exhibits distinct regional characteristics, with significant heterogeneity in emissions among regions. (2) With advancements in technology and economy, China's carbon emission intensity has shown a downward trend, albeit with a U-shaped fluctuation. (3) During the sample period, the contribution of Theil index to carbon emission intensity decreased first and then increased. (4) From a geographical perspective, carbon emissions exhibit a pattern characterized by "high in the east, low in the west, dense in the north and sparse in the south". Therefore, establishing a sound regional carbon reduction cooperation mechanism and promoting green development tailored to local conditions have become the main direction for advancement.

**Keywords: Carbon emission intensity; Extended Kaya model; Standard deviation ellipse model; Theil index model; Kernel density model**

---

## 1. Introduction

China's rapid economic growth has been largely attributed to the development of traditional manufacturing industries. However, this growth model is characterized by high pollution and high resource input, representing an extensive approach to economic development, leading to ongoing issues including air pollution and environmental degradation. According to the IEA, China's carbon emissions in 2022 exceeded 11.14 billion tons, indicating a slight 0.2% reduction from the previous year, yet the absolute amount still commands considerable attention. In order to avoid climate crisis, in 2022, the Chinese government formally proposed to the United Nations the "dual carbon" goal of "carbon peak by 2030 and carbon neutrality by 2060" (Yuan et al., 2023). In addition, the report of the 20th National Congress of the Communist Party of China repeatedly stressed that more measures should be taken to achieve the "dual carbon" goal (Chang, 2022). Therefore, to facilitate the achievement of the "dual carbon" targets, it has become an urgent issue to conduct a comprehensive investigation on the spatial distribution pattern of carbon emissions across provinces in China and clarify the dynamic evolution of provincial carbon emissions.

Carbon emission has an important impact on economic development (Li et al., 2023; Zheng et al., 2023; Luo et al., 2023; Liu et al., 2024; Xu et al., 2023; Xu et al., 2024). Some scholars analyzed the carbon emission control mechanism from the perspectives of green building engineering, energy productivity, digitalization, waterway network, manufacturing transformation, technological innovation efficiency, sewage treatment, residential land transfer, etc. (Zhang et al., 2019; Zhang et al., 2023; Sun et al., 2024; Chen et al., 2024; Zhao et al., 2024; Qiu et al., 2024; Zhao et al., 2024; Liu, et al., 2024; Liu, et al., 2024). These studies provide significant references for the investigation of carbon emission issues.

Many scholars at home and abroad have paid attention to the efficiency of carbon emission intensity. Common methods involve parametric estimation or non-parametric estimation (Tao et al., 2022; Mohammad et al., 2021; Andrea et al., 2022; Blanchard, 2021; Cai, 2023; Liu, 2024). Wu et al. (2022) calculated the carbon emission efficiency of crops in 30 provinces in China from 2001 to 2019 based on an extended relaxation-based measurement method. Zhang and Xi (2023) constructed a three-dimensional evaluation index system to evaluate the ecological environment and agricultural development in China's provinces based on the stage. The efficiency SBM model measures the efficiency of urban carbon emissions. Li et al. (2023) measured the carbon emission efficiency of the urban agglomerations in the Yangtze River Economic Belt, using the super-efficiency SBM model of undesirable output. Dussaux et al. (2023) analyzed the impact of third-country imports on France's domestic carbon intensity based on the shift-share instrumental variable method. Wei and Hengye (2022) utilized panel data to examine the impact of the first-order term of carbon emissions on carbon emission intensity. Zhang

---

32 et al. (2022) used the super-efficiency three-stage data envelopment analysis model to measure the carbon  
33 emission intensity of Chinese agriculture from 2000 to 2019. Most of the aforementioned studies are based on  
34 the classic DEA model, proposing a multi-stage efficiency measurement method; however, these studies are  
35 primarily focused on the comparison of relative efficiency. Additionally, some scholars have used the  
36 stochastic frontier analysis models to measure carbon emission efficiency (Guo and Liang, 2022; Xu, 2022).  
37 Furthermore, there are scholars who have concentrated on the impact of environmental factors on carbon  
38 emission intensity, mainly employing econometric and statistical analysis models (Andrea et al., 2021; Li et al.,  
39 2023).

40 At present, the spatial analysis of carbon emissions has become a research frontier. Existing literature mainly  
41 focuses on issues such as carbon emission performance and characteristics, with primary research methods  
42 including trend analysis, Gini coefficient, and standard deviation ellipse. (Najul et al., 2022; Liu et al., 2022; Wang  
43 et al., 2023). On this basis, some scholars have used global spatial autocorrelation coefficients to reveal the spatial  
44 correlation of carbon emissions (Wei and Dong, 2022; Zhou et al., 2023). In addition, some scholars have  
45 employed LISA time path, kernel density estimation, center-standard deviation ellipse, and other methods to  
46 analyze the spatiotemporal evolution characteristics of carbon emissions (Zhao et al., 2021; Liu and Wei, 2022;  
47 Zhang, 2023). Specifically, in terms of carbon emission performance, existing studies have indicated that China's  
48 carbon emissions have shown a fluctuating upward trend as a whole, with performance values changing from a  
49 low-value concentration and skewed distribution to a medium-value concentration and symmetric distribution  
50 (Cheng et al., 2023). Besides, China's carbon emissions demonstrate regional imbalances, with carbon emission  
51 performance presenting significant spatial disparities and pronounced spatial correlation characteristics, showing  
52 a distribution pattern of east > central > west (Hao et al., 2022). The polarization effect is significant in the  
53 Beijing-Tianjin-Hebei region and Yellow River basins. (Wang et al., 2023).

54 In summary, many scholars have conducted studies on the spatial distribution pattern and temporal  
55 evolution of carbon emissions at the regional, provincial (district and city), or county scale in China, yielding  
56 substantial results. However, the focus of these studies has been largely confined to specific regions, and the  
57 conclusions drawn from research data that is limited in scope and duration are inherently constrained, thereby  
58 precluding a holistic examination of the dynamic progression of China's carbon emission intensity. In view of  
59 this, the main objective of this paper is to analyze China's carbon emission intensity and its spatial characteristics.  
60 To clarify, this paper uses the standard deviation ellipse method to investigate the distribution characteristics of  
61 carbon emission spatial concentration in 30 provinces of China from 2005 to 2022. Subsequently, the Theil index

62 is applied to characterize spatial differences, and ultimately, the kernel density model is employed to analyze the  
63 evolving trends.

64 The marginal contribution of this article lies in (1) Regarding the sample data, this study leverages carbon  
65 emission data from the CEADs database for China's 30 provincial regions to conduct a thorough examination of  
66 the distribution characteristics of China's carbon emission intensity. (2) In terms of research methods, this paper  
67 adopts the multi-method systematic analysis paradigm, using carbon emission intensity measurement, standard  
68 deviation ellipse, Theil index, kernel density and other models to systematically analyze the spatial effects of  
69 carbon emission intensity. (3) Concerning research value, the research conclusions of this article contribute to  
70 exploring carbon reduction pathways for Chinese provincial regions under diverse evolving trends, offering  
71 decision-making insights for the formulation of scientific inter-provincial carbon neutrality action plans that are  
72 adapted to China's new development pattern, thereby facilitating the achievement of China's dual carbon targets.

## 73 **2. Materials and Methods**

### 74 **2.1 Construction of Carbon Emission Intensity Measurement Model**

75 Due to the lack of publicly disclosed carbon emission data from China's official sources,, most scholars  
76 index carbon emissions based on the Kaya model, with a principal focus on factors including economy,  
77 demography, and significant fuel consumption. The Kaya model was first proposed by Professor Yoichi Kaya,  
78 who has provided a specialized introduction to the method at a meeting of the United Nations Climate Change  
79 Conference. The model offers advantages including simple calculation, and elimination of the interference of  
80 residual and disturbance terms, effectively explaining the main factors affecting carbon emissions (Lv et al.,  
81 2016). The expression for calculating carbon emissions using the Kaya model is as follows (Du et al., 2022) :

82

$$83 \quad Q = p \times \left(\frac{Q_p}{E_p}\right) \times \left(\frac{E_p}{P_{GD}}\right) \times \left(\frac{P_{GD}}{P}\right) \quad (2-1)$$
$$= p \times s \times i \times e$$

84 In the above equation,  $Q$  represents total carbon emissions,  $E = E_p$  represents energy consumption,

85  $G = P_{GD}$  represents gross domestic product,  $P$  represents population size,  $s = \frac{Q_p}{E_p}$  represents carbon

86 dioxide emissions per unit of GDP,  $i = \frac{E_p}{P_{GD}}$  represents energy input per unit of GDP, and  $e = \frac{P_{GD}}{P}$

87 represents GDP per capita.

88 Further, according to the extended identity of the LMDIM obtained from the Kaya model, the residual value

89 of the decomposition is obtained (Dai et al., 2015):

90 The residual value of the extended identity equation LMIDIM without decomposition

91

92

$$\begin{aligned} \Delta Q &= Q_x - Q_y = \Delta Q_{pe} + \Delta Q_{ee} + \Delta Q_{ie} + \Delta Q_{se} \\ \Delta Q_{pe} &= \frac{N_x - N_y}{\ln N_x - \ln N_y} \ln \frac{p_x}{p_y}, \\ \Delta Q_{ee} &= \frac{Q_x - Q_y}{\ln Q_x - \ln Q_y} \ln \frac{e_x}{e_y}, \\ \Delta Q_{ie} &= \frac{Q_x - Q_y}{\ln Q_x - \ln Q_y} \ln \frac{i_x}{i_y}, \\ \Delta Q_{se} &= \frac{Q_x - Q_y}{\ln Q_x - \ln Q_y} \ln \frac{s_x}{s_y}, \end{aligned} \quad (2-2)$$

94 Where  $\Delta Q$  represents the difference in carbon emissions, and  $Q_x$  and  $Q_y$  represent the carbon  
95 emissions in year  $x$  and year  $y$ , respectively.  $\Delta Q_{pe}$  represents population size,  $\Delta Q_{ee}$  represents economic  
96 output effect, and  $\Delta Q_{ie}$  and  $\Delta Q_{se}$  represent energy substitution effect and energy structure effect respectively.

97 Carbon emission intensity usually refers to the amount of carbon emissions per unit of GDP. According to  
98 the Kaya model and its extended-expression, energy consumption and its effect function can be calculated.  
99 Therefore, the calculation formula for provincial carbon emission intensity is as follows (Zhao et al., 2017):

$$100 \quad PCEI_{ij} = \frac{Q_{provEmission_{it}}}{GDP_{it}} \quad (2-3)$$

101 Where,  $PCEI_{ij}$  represents the carbon emission intensity of research object  $i$ ,  $Q_{provEmission_{it}}$   
102 represents the carbon emission of research object  $i$  in year  $t$ , and  $GDP_{it}$  represents the gross product of  
103 research object  $i$  in year  $t$ .

## 104 2.2 Construction of SDE model considering carbon emission differences

105 It is necessary to analyze the characteristics of carbon emission intensity from the perspective of space. In  
106 this paper, the standard deviation ellipse model (SDE) will be constructed. The strength of this model lies in  
107 its capacity to effectively distinguish the overall and discrete distributions of different factors in multiple  
108 directions (Xu et al., 2023).

109 According to relevant research, the standard deviation ellipse model can effectively calculate parameters

110 including the distribution center, long-axis standard deviation, short-axis standard deviation, and azimuth angle  
 111 of carbon emission intensity can be effectively calculated. The calculation formula is as follows (Liu et al., 2019):

112 (1) Spatial distribution center of gravity:

113

$$\bar{X}_c = \frac{\sum_{i=1}^n \omega_i x_i}{\sum_{i=1}^n \omega_i} \quad (2-4)$$

114

$$\bar{Y}_c = \frac{\sum_{i=1}^n \omega_i y_i}{\sum_{i=1}^n \omega_i}$$

115 (2) The standard deviations along the X-axis and Y-axis directions are, respectively:

116

$$\sigma_x = \sqrt{\frac{\sum_{i=1}^n (w_i \bar{x}_i \cos \theta - w_i \bar{y}_i \sin \theta)^2}{\sum_{i=1}^n w_i^2}} \quad (2-5)$$

117

118 (3) Azimuth angle:

$$\tan \theta = \frac{(\sum_{i=1}^n w_i^2 \bar{x}_i^2 - \sum_{i=1}^n w_i^2 \bar{y}_i^2) + \sqrt{(\sum_{i=1}^n w_i^2 \bar{x}_i^2 - \sum_{i=1}^n w_i^2 \bar{y}_i^2)^2 + 4 \sum_{i=1}^n w_i^2 \bar{x}_i \bar{y}_i}}{2 \sum_{i=1}^n w_i^2 \bar{x}_i \bar{y}_i} \quad (2-6)$$

120 In the above formula,  $\bar{x}_i, \bar{y}_i$  represent the relative coordinates of the distance distribution center of gravity  
 121 of the spatial location  $(x_i, y_i)$  respectively.  $w_i$  stands for weight.  $\theta$  is the azimuth of the standard  
 122 deviation ellipse.

### 123 2.3 Construction of Theil index model of carbon emission intensity decomposition

124 This paper primarily investigates the spatial characteristics of carbon emission intensity at the provincial  
 125 level. Since carbon emission intensity has eliminated the regional economic and demographic heterogeneities,  
 126 the Theil index is commonly utilized to measure it. (Song and Lv, 2017).

127 Theil index T is calculated using GDP proportion weighting. By conducting a first-order decomposition of

128 the Theil index, the total national carbon emission difference can be decomposed into inter-regional and intra-  
 129 regional differences across seven major regions: South China, Central China, Northeast China, Southwest China,  
 130 North China, East China, and Northwest China. The formula for the total difference Theil index is as follows  
 131 (Meng et al., 2018; Ren et al., 2022):

$$132 \quad T_p = \sum_i \sum_j \left( \frac{Y_{ij}}{Y_i} \right) \log \left( \frac{Y_{ij}/Y}{P_{ij}/P} \right) \quad (2-7)$$

133  
 134 Where,  $Y_{ij}$  is the GDP of the  $j$  province in Region  $i$ .  $Y_i$  is the GDP of region  $i$ ,  $P_{ij}$  is the carbon  
 135 emission intensity of the  $j$  province in Region  $i$ .  $P_i$  is the total carbon emission intensity of region  $i$ .  $P$   
 136 is the total carbon emission intensity of the province. The inter-provincial differences that define region  $i$  are:

$$137 \quad T_p = \sum_j \left( \frac{Y_{ij}}{Y_i} \right) \log \left( \frac{Y_{ij}/Y}{P_{ij}/P} \right) \quad (2-8)$$

138 Then the total difference can be decomposed by  $T_p$  into:

$$139 \quad \begin{aligned} T_p &= \sum_i \left( \frac{Y_i}{Y} \right) T_{p_i} + \sum_j \left( \frac{Y_j}{Y} \right) \log \left( \frac{Y_j/Y}{P_j/P} \right) \\ &= T_{WR} + T_{BR} \end{aligned} \quad (2-9)$$

140 Where  $T_{WR}$  is the difference within the region,  $T_{BR}$  is the difference among regions.

## 141 2.4 Construction of kernel density estimation model for analyzing spatio-temporal 142 characteristics

143 To illustrate the continuous evolving trend of carbon emission structure in space, kernel density analysis is  
 144 utilized to interpret the spatiotemporal evolution of carbon emission within Chinese provincial regions. Kernel  
 145 density estimation method is a method of estimating unknown density function in probability theory (Wang and  
 146 Wang, 2015; Wang and Huang, 2023).

147 The basic assumption of this method is that  $X_1, X_2, X_3, \dots, X_n$  follows  $n$  independent and equally  
 148 distributed sample points, let the corresponding density function be  $f(x)$ ,  $f(x)$  is unknown and needs to be  
 149 estimated by sample. The empirical distribution function of  $X_1, X_2, X_3, \dots, X_n$  is (Cui and Li, 2021; Lee et  
 150 al., 2022; Luo et al., 2020):

$$151 \quad f(x) = \frac{1}{n} \{X_1, X_2, \dots, X_n\} \quad (2-10)$$



152 The density estimation function can be obtained as follows:

$$\begin{aligned} f_h(x) &= \frac{[F_n(x+h_n) - F_n(x-h_n)]}{2h} \\ &= \int_{x-h_n}^{x+h_n} \frac{1}{h} K\left(\frac{t-x}{h_n}\right) dF_n(t) \quad (2-11) \\ &= \frac{1}{nh} \sum_{i=1}^n K\left(\frac{x_i-x}{h_n}\right) \end{aligned}$$

154 Where  $n$  is the total amount of carbon emission intensity data at provincial level;  $h$  is the bandwidth;  
155  $k()$  is the kernel function;  $x_i$  is provincial carbon emission intensity, which belongs to independent and  
156 homogeneous distribution.

### 157 2.5 Sources of research data

158 The carbon emission data in this paper are mainly from CEAD's database ([www.ceads.net](http://www.ceads.net)), which primarily  
159 calculates carbon emissions based on the Kaya model and its improved methodologies. The study targets 30  
160 provinces (municipalities and autonomous regions) in China. Tibet, Hong Kong, Macau and Taiwan are not  
161 considered due to lack of statistical data. Data for other variables are derived from authoritative publications such  
162 as China Statistical Yearbook and China Environmental Statistical Yearbook. Some missing data were completed  
163 by linear interpolation. In addition, due to the lag of the statistical yearbook, part of the 2022 data were  
164 supplemented by regression analysis.

## 165 3. Results

### 166 3.1 Carbon emission intensity measurement results

167 Based on the Kaya model and its improved model, statistical data were collected, and using MATLAB  
168 tools, the carbon emission intensity of 30 provincial regions in China from 2005 to 2022 can be calculated as  
169 shown in Table 1.

170 From the results, The intensity of carbon emissions shows a trend of first increasing and then decreasing.  
171 Although from 2005 to 2006, the intensity of carbon emissions remained relatively stable at 14.5 billion tons  
172 per billion tons, China's carbon emissions intensity has been steadily declining since a significant decrease in  
173 2007, indicating that China's carbon emissions intensity indicator has been declining year by year due to  
174 technological progress and economic growth. 2020 and 2022 saw rebound in carbon emission intensity, which  
175 could be primarily attributed to two factors: the relaxation of environmental policies by the Chinese

176 government in response to the COVID-19 from 2019, and the consequent surge in coal power generation due

177 to electricity shortages. Table 1: Carbon emission intensity of China's provinces (2005-2022)

Province	2005	2006	2007	2008	2009	2010	2011	2012	2013	2014	2015	2016	2017	2018	2019	2020	2021	2022
Beijing	1.68	1.47	1.26	1.13	1.06	0.93	0.75	0.69	0.57	0.54	0.49	0.42	0.38	0.35	0.32	0.32	0.33	0.35
Tianjin	3.93	3.74	3.39	2.71	2.64	2.70	2.49	2.25	2.12	1.92	1.85	1.66	1.52	1.47	1.41	2.10	2.26	1.51
Hebei	6.57	6.18	5.58	4.97	4.92	4.50	4.28	4.02	3.84	3.51	3.51	3.26	3.01	2.91	2.71	3.23	3.64	2.75
Shanxi Province	13.89	13.36	11.05	8.73	8.74	7.53	6.78	6.60	6.60	6.70	7.85	7.70	6.69	6.50	6.44	8.07	8.65	7.07
Inner Mongolia	8.85	12.11	8.20	8.07	7.72	7.38	7.98	7.49	6.73	6.46	6.01	5.71	5.56	5.89	6.13	8.43	7.52	7.62
Liaoning	6.73	6.29	5.52	4.89	4.79	4.84	4.40	4.17	3.74	3.59	3.44	3.45	3.34	3.28	3.38	3.82	4.42	4.65
Jilin	6.28	5.71	4.77	4.55	4.14	3.92	3.71	3.27	2.90	2.72	2.31	2.19	2.07	2.08	2.06	2.01	2.12	2.32
Heilongjiang	5.24	4.98	4.66	4.24	4.38	4.13	3.70	3.50	3.08	3.04	2.90	2.87	2.78	2.72	2.70	2.73	2.77	2.88
Shanghai	2.50	2.16	1.82	1.70	1.57	1.51	1.39	1.28	1.25	1.05	0.99	0.88	0.82	0.74	0.72	0.76	0.79	0.81
Jiangsu	2.65	2.47	2.18	1.86	1.75	1.62	1.59	1.47	1.37	1.25	1.17	1.12	1.00	0.92	0.88	0.89	0.91	0.93
Zhejiang	2.30	2.21	2.02	1.81	1.75	1.57	1.43	1.28	1.22	1.12	1.05	0.96	0.90	0.80	0.76	0.77	0.78	0.79
Anhui Province	3.46	3.24	2.96	2.83	2.73	2.37	2.07	1.92	1.86	1.75	1.66	1.50	1.38	1.25	1.16	1.18	1.20	1.22
Fujian	2.05	1.96	1.77	1.58	1.64	1.51	1.45	1.27	1.12	1.15	1.03	0.88	0.81	0.78	0.76	0.77	0.79	0.81
Jiangxi	2.97	2.72	2.42	2.05	1.95	1.84	1.65	1.50	1.45	1.34	1.31	1.21	1.12	1.04	0.98	0.99	1.01	1.03
Shandong Province	4.47	4.31	3.91	3.48	3.33	3.20	2.93	2.80	2.48	2.47	2.50	2.47	2.37	2.22	2.15	2.16	2.19	2.23
Henan Province	4.15	4.02	3.60	3.10	2.93	2.68	2.55	2.17	1.97	1.82	1.60	1.45	1.28	1.15	0.99	0.93	0.97	1.00
Hubei Province	3.74	3.60	3.18	2.57	2.41	2.24	2.07	1.83	1.41	1.28	1.13	1.03	0.94	0.87	0.85	0.83	0.87	0.91
Hunan Province	3.39	3.09	2.86	2.32	2.16	1.88	1.73	1.52	1.33	1.18	1.06	1.00	0.93	0.88	0.80	0.76	0.82	0.86
Guangdong Province	1.75	1.65	1.46	1.31	1.32	1.27	1.18	1.08	1.01	0.93	0.86	0.80	0.75	0.71	0.66	0.63	0.64	0.66
Guangxi	2.64	2.44	2.29	1.97	1.99	2.01	2.05	2.05	1.88	1.71	1.47	1.40	1.35	1.28	1.25	1.27	1.30	1.32
Hainan	1.84	2.38	3.64	3.16	3.06	2.68	2.59	2.39	1.98	1.98	2.01	1.78	1.57	1.52	1.44	1.59	1.75	1.86
Chongqing	3.10	2.98	2.65	2.25	2.14	1.95	1.76	1.53	1.18	1.12	0.90	0.82	0.76	0.71	0.66	0.65	0.68	0.71
Sichuan	3.19	2.98	2.69	2.34	2.36	2.01	1.66	1.52	1.41	1.34	1.09	0.98	0.84	0.73	0.72	0.75	0.79	0.85
Guizhou	8.53	8.39	7.21	6.00	5.97	5.14	4.57	4.17	3.66	3.07	2.67	2.50	2.18	1.78	1.67	1.76	1.87	1.96
Yunnan Province	5.05	4.75	4.00	3.47	3.45	3.10	2.60	2.31	1.98	1.63	1.38	1.25	1.18	1.16	1.09	1.04	1.09	1.13
Shaanxi	4.70	4.78	4.22	3.71	3.62	3.48	3.11	3.08	2.91	2.80	2.69	2.58	2.36	2.07	2.08	2.20	2.27	2.32
Gansu Province	6.94	6.27	5.75	5.10	4.73	4.36	4.13	3.80	3.52	3.27	3.15	2.87	2.73	2.59	2.43	2.43	2.47	2.51
Qinghai Province	5.39	5.40	5.16	4.53	4.40	3.61	3.56	3.81	3.74	3.24	2.74	2.85	2.50	2.19	2.02	2.05	2.13	2.21
Ningxia	12.71	11.81	10.21	8.78	8.68	8.28	8.97	8.73	8.51	8.15	8.11	7.49	8.00	8.13	8.28	8.45	8.58	8.70
Xinjiang	6.09	5.93	5.45	5.10	5.82	5.15	5.00	5.09	5.15	5.19	5.33	5.38	4.94	4.48	4.49	4.76	4.96	5.08

178 As shown in Figure 1, from the regional perspective, since 2005, the carbon emission intensity in eastern

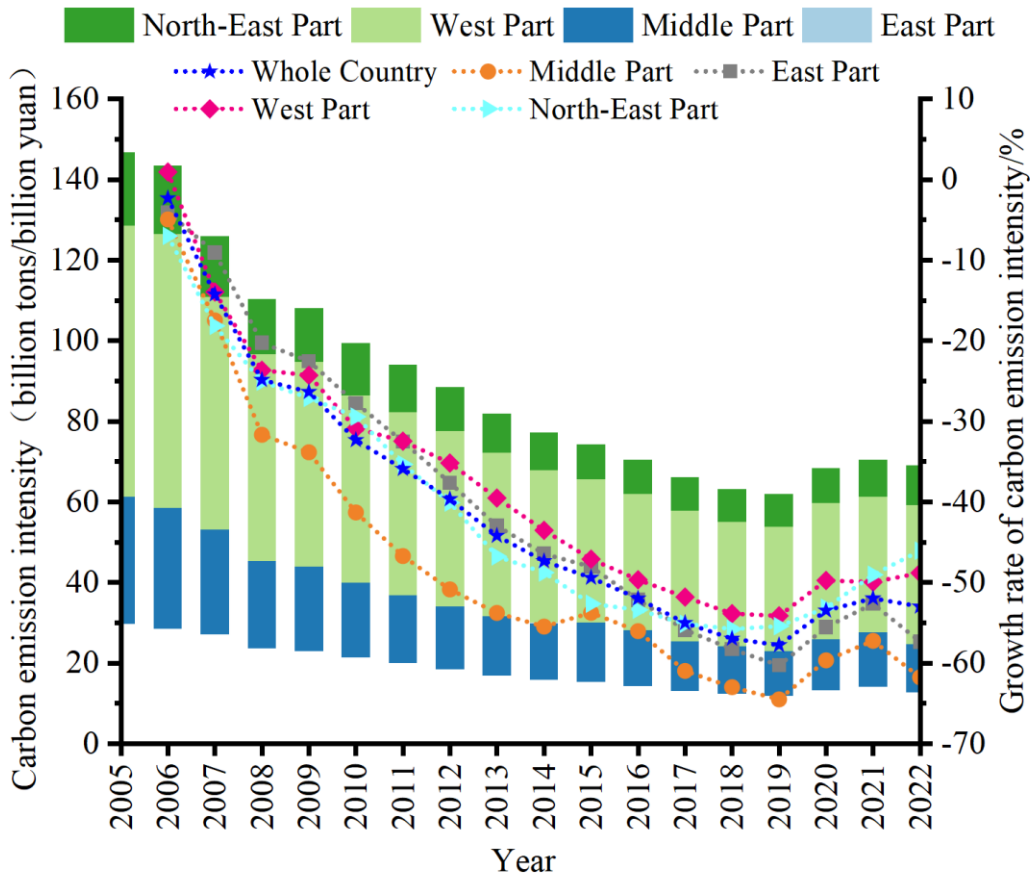
179 region has decreased first, reaching a low point in 2019, with an emission volume of 1.18 billion tons/100

180 million yuan, accounting for about 19% of the country's total, but rebounding to 1.41 billion tons/100 million

181 yuan in 2021. During the sample investigation period, the carbon intensity in the central and western regions

182 both showed significant decreases, from 3.16 billion tons/100 million yuan to 1.12 billion tons/100 million

183 yuan and from 6.72 billion tons/100 million yuan to 3.08 billion tons/100 million yuan, accounting for 18%  
 184 and 50% of the country's total emissions, respectively, rebounding to 1.35 billion tons/100 million yuan and  
 185 3.36 billion tons/100 million yuan in 2021. The change was most significant in Northeast China, where carbon  
 186 emissions dropped from 1.82 billion tons per billion yuan in 2015 to 810 million tons per billion yuan in 2019,  
 187 and finally rebounded to 990 million tons per billion yuan in 2022. Some regions experienced fluctuations in  
 188 2022, with the eastern and central regions dropping to 1.27 billion tons per billion yuan and 1.21 billion tons  
 189 per billion yuan respectively.



190  
 191  
 192

Figure 1 Growth rate of carbon emission intensity in different regions

193 **3.2 Results of carbon emission intensity based on the standard deviation ellipse model**

194 By ARCGIS calculation, typical time points are selected for analysis. According to Figure 2, the range of  
 195 change in the distribution of the centroid of the ellipse is [110° 0' ~110° 43' ] E, [ 35° 52' ~37° 23' ]  
 196 N. Compared with the geometric center of China (103°E, 36°N), this time the centroid is shifting to the southeast.  
 197 By examining the specific trajectory and direction of the change in the centroid of the standard deviation ellipse,  
 198 within the scope of this investigation, the central point of China's carbon emission distribution moved from

199 Xiangning County towards the northwest to Yonghe County, and then gradually shifted to the northeast.  
 200 Consequently, the central point of carbon emissions is shifting to the northwest.

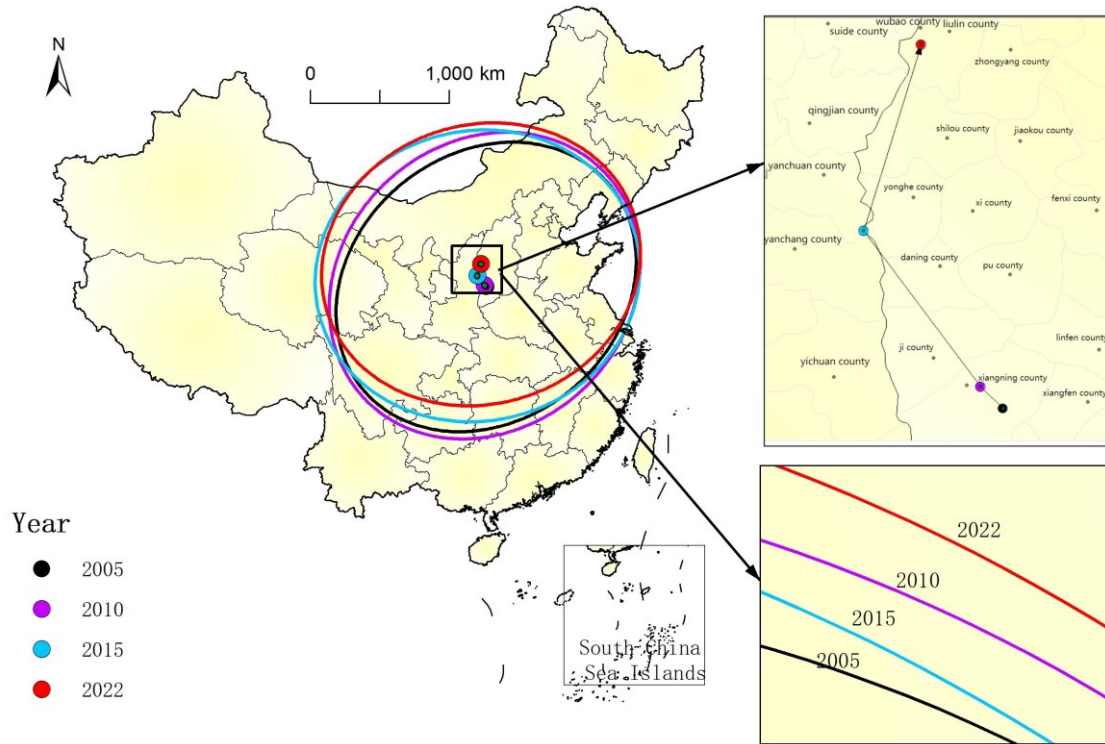


Figure 2. Results of centroid-standard deviation ellipse of carbon emission intensity  
 Standard Map of China - Review No. GS (2020) 4619

201

202 Figure 2. Results of centroid-standard deviation ellipse of carbon emission intensity

### 203 3.3 Decomposition results of carbon emission intensity based on Theil index

204

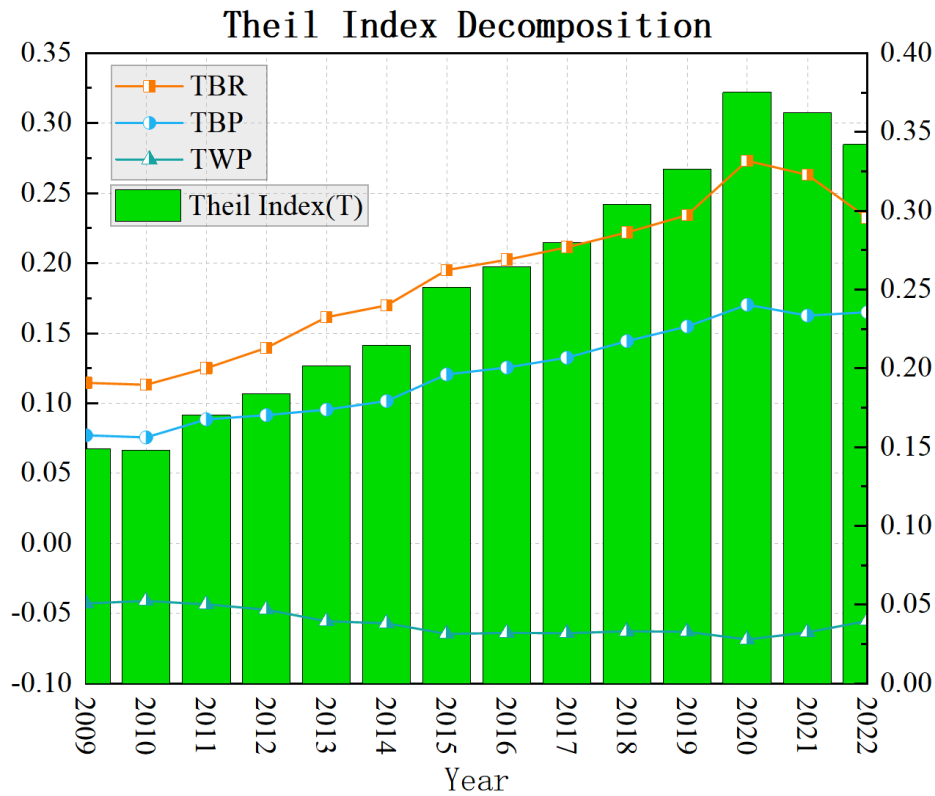
205 The previous analysis shows significant differences in carbon emissions among regions, with the  
 206 distribution of carbon emission intensity demonstrating pronounced regional attributes. This warrants an in-  
 207 depth examination of the factors contributing to the observed inter-regional emission differences. This article  
 208 introduces the Theil index to measure the regional differences in carbon emission intensity. Compared to other  
 209 methods, the Theil index makes it possible to observe the change between entities and their overall impact more  
 210 clearly.

211 Through the first-order decomposition of Theil index, seven regional differences and inter-provincial  
 212 differences in China's carbon emissions were analyzed. According to Table 2 and Figure 3, it can be seen that  
 213 during the sample investigation period, China's carbon emission intensity differences showed an upward trend,  
 214 from 0.1393 in 2010 to 0.2475 in 2019. The intra-provincial variation fluctuates around 0.15, which is the most  
 215 important source of overall variation. The contribution rate of intra-group differences to the overall trend is

216 increasing. According to the data from 2009 to 2022, the value of TBR is greater than that of TBP, and the  
 217 value of TWP is negative. For example, the TBR value, TBP value and TWP value in 2022 are 0.2323, 0.1651  
 218 and -0.0553 respectively, and the Theil index value is 0.3421. Changes of Theil index in Figure 2 displays that  
 219 the Theil index curve keeps increasing from 2009 to 2020, and slightly decreases from 2021 to 2022. This  
 220 shows that the overall difference in carbon emission intensity has generally maintained an increasing trend.

221 Table 2 Decomposition value of the Theil index for carbon emissions across provincial regions in China

Years	TBR	TBP	TWP	Theil index
2009	0.1147	0.0772	-0.0428	0.1490
2010	0.1133	0.0757	-0.0411	0.1479
2011	0.1251	0.0886	-0.0435	0.1702
2012	0.1396	0.0916	-0.0473	0.1839
2013	0.1615	0.0956	-0.0555	0.2015
2014	0.1700	0.1017	-0.0570	0.2147
2015	0.1952	0.1207	-0.0646	0.2513
2016	0.2025	0.1257	-0.0638	0.2644
2017	0.2114	0.1326	-0.0641	0.2798
2018	0.2220	0.1445	-0.0627	0.3038
2019	0.2344	0.1549	-0.0631	0.3262
2020	0.2732	0.1705	-0.0685	0.3751
2021	0.2631	0.1627	-0.0634	0.3624
2022	0.2323	0.1651	-0.0553	0.3421



222

223 Figure 3. Decomposition value of the Theil index for carbon emissions across provincial regions in China –

224

Line Chart

225 **3.4 Spatial and temporal evolution results of carbon emission intensity based on kernel**  
 226 **density estimation model**

227 The evolution of carbon emission intensity is essentially a dynamic process of aggregation and diffusion  
 228 among crucial regions. However, it is difficult for the above research to visually express the carbon emission  
 229 change path in different provinces. Therefore, kernel density model is introduced for analysis.

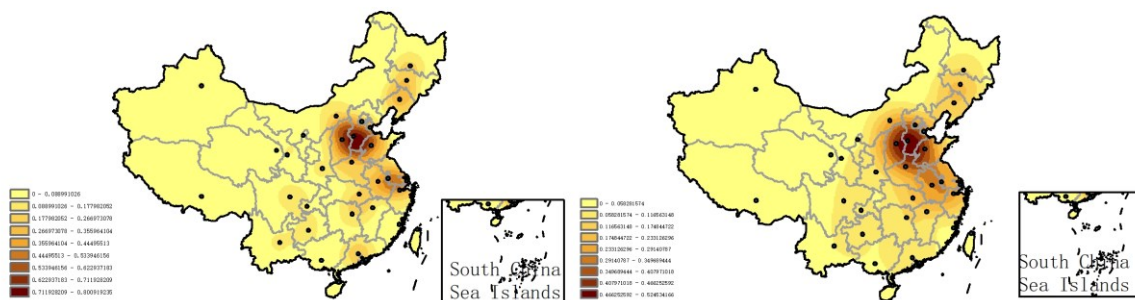
230 As shown in Figure 4, according to the analysis of the evolution, the multi-scale bandwidth can reflect the  
 231 spatiotemporal evolution of carbon emission intensity. On the whole, the Kernel density on the map is higher in  
 232 the east than in the west, dense in the north and sparse in the south. In addition, there are also significant  
 233 differences within the region, and the results are consistent with the previous findings.

234

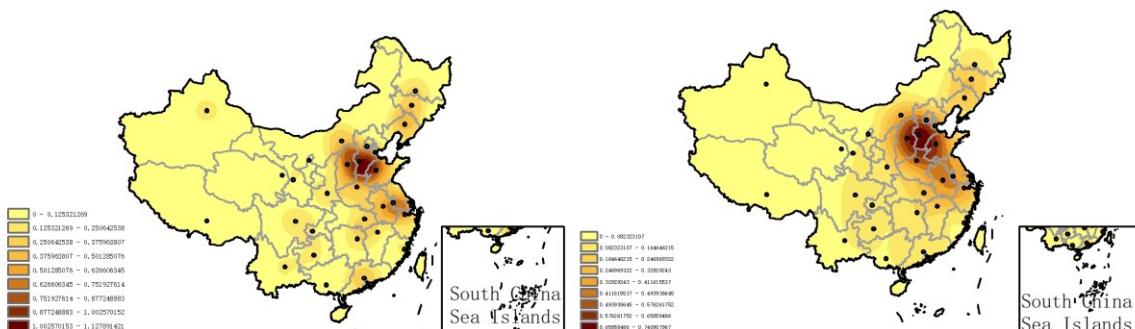
235

236

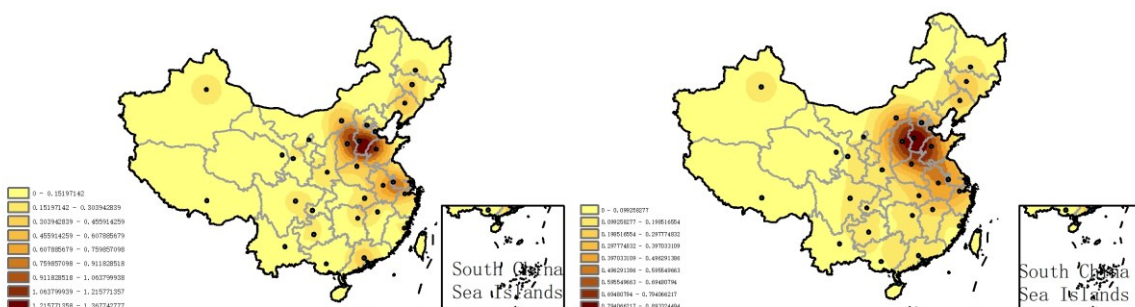
2005



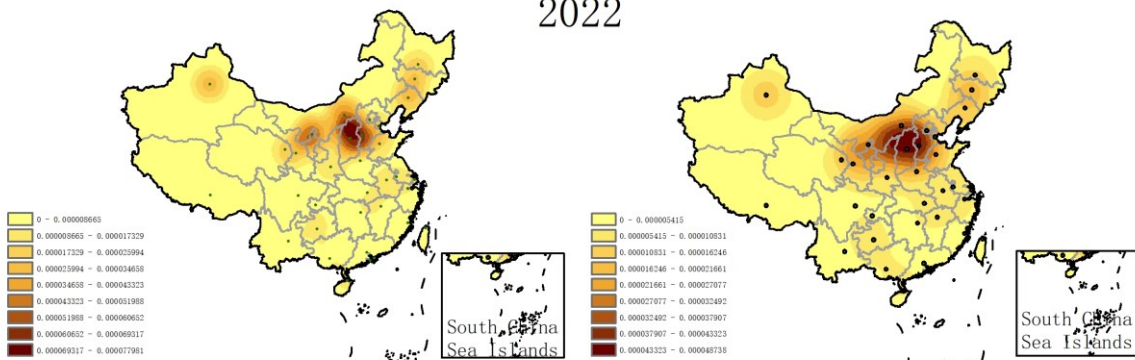
2010



2015



2022



237

238

Figure 4: Spatial distribution pattern of carbon emission intensity across provincial regions in China in

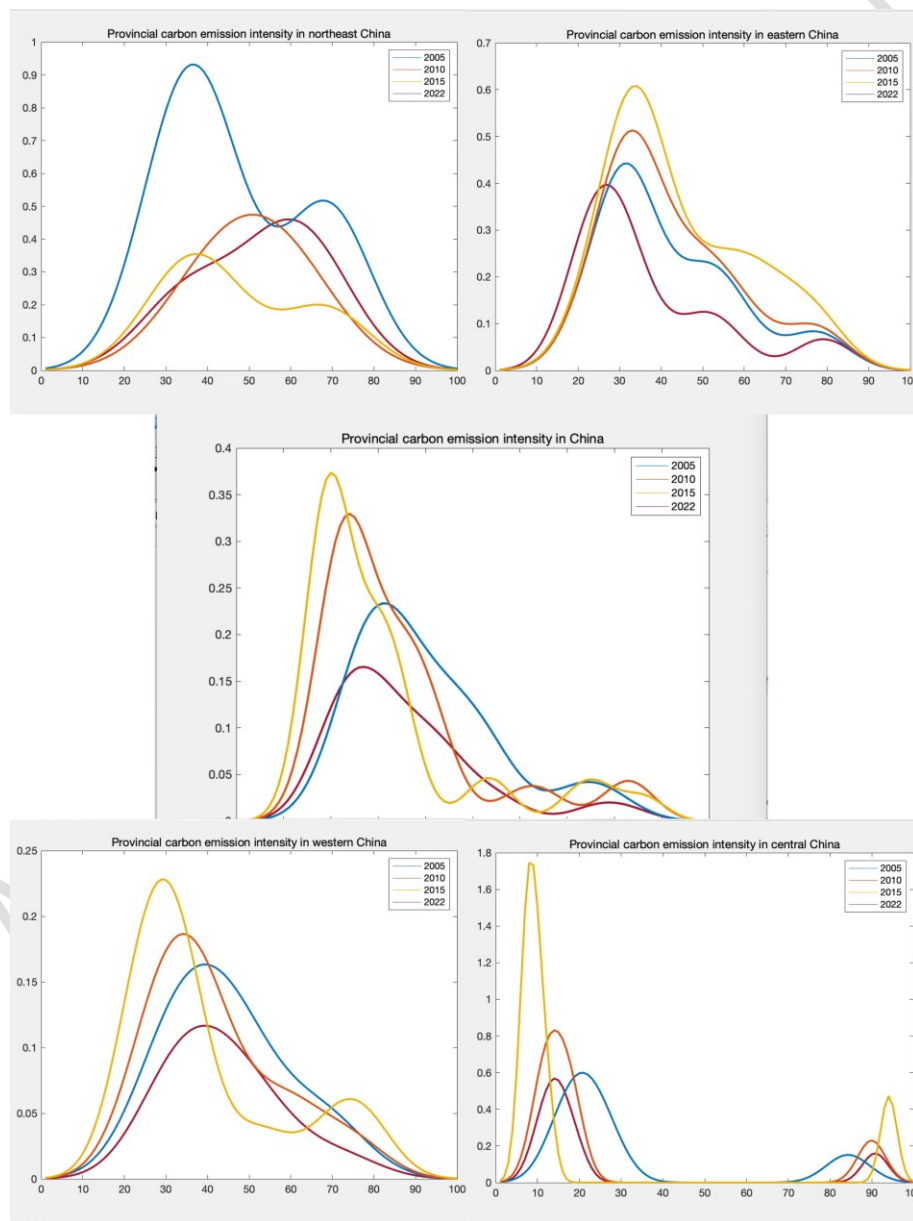
239

2005, 2010, 2015, and 2022

240

Standard Map of China - Drawing Review No. GS (2020) 4619

241 Further, the variations of regional Kernel density curves in 2005, 2010, 2015 and 2022 were plotted  
 242 respectively, as shown in Figure 5. Taking the central region as an example, the Kernel density curve in 2022  
 243 first increased and then decreased, and subsequently increased again before decreasing, showing the  
 244 characteristics of "U-shaped" and "inverted U-shaped" changes, with consistent patterns observed in the year  
 245 2005, 2010, and 2015. The national trend, along with those of the eastern, western, and northeastern regions, has  
 246 exhibited similar patterns of change. Consequently, an examination of evolution trend of carbon emission  
 247 intensity across China and its four regions, with focus on the curve's positioning, span, and peak value, indicates  
 248 pronounced spatial and temporal heterogeneity in carbon emission intensity.



269

270 Figure 5 Distribution of carbon emission intensity across provincial regions in China

271 **4. Discussion**



---

#### 272 4.1 Further discussion on changes in carbon emission intensity

273 The results of carbon emission intensity were calculated based on the Kaya model and its improved  
274 model. To compare the trends in different time series from 2005 to 2022 in China, the map in Figure 6 was  
275 drawn using ArcGIS software.

276 Referring to relevant studies (Kamani et al., 2023), as shown in Fig6, in terms of the growth rate of carbon  
277 intensity, the trend in the growth rate of carbon emissions across China's provincial regions has been on a  
278 downward trajectory from 2006 to 2019.. Furthermore, aside from the western region experiencing a positive  
279 growth rate in 2006, all other regions have shown a negative growth in carbon intensity in all subsequent years.  
280 From 2020 to 2022, the growth rate of carbon emissions saw a resurgence. Regarding the growth rate of  
281 carbon intensity, except for a fluctuating rebound in the central region in 2015, all other areas showed a  
282 downward trend. Based on the results, it can be seen that the intensity of carbon emissions is significantly  
283 affected by economic growth and policy measures. In 2020, when the Chinese government proposed the  
284 strategic goal of "carbon peak by 2030", the intensity of carbon emissions rebounded, illustrating that 2020 was  
285 a significant turning point.

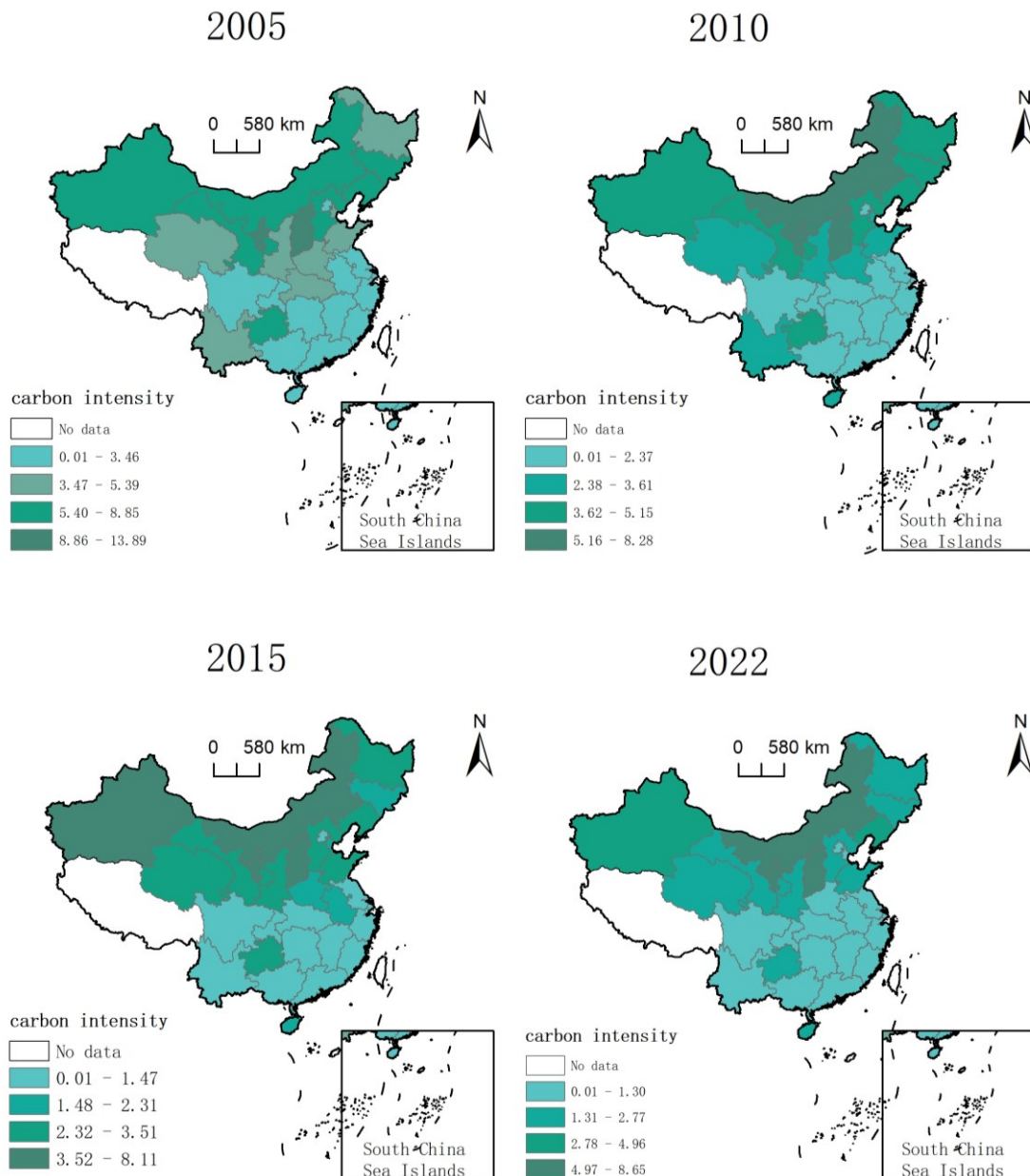


Figure 6 Carbon intensity map for 2005/2006/2015/2022  
Standard Map of China – Approval No. GS (2020) 4619

286

287

## Figure 6 Spatial distribution of carbon emission intensity across different provinces

288

### 4.2 Discussion on the decomposition of carbon emission intensity based on Theil index

289

Theil index is instrumental in assessing regional differences in carbon emissions. Beyond analyzing the differences in carbon emission intensity at the provincial level, it is also necessary to adopt a regional clustering method to compare the spatial differences in China's carbon emissions (Kamani, 2023). According to the clustering results, the sample data is reclassified to obtain the carbon emission intensity of different regions.

292

293

As shown in Table 3, during the study period, the overall difference in carbon emission intensity among the seven regions has increased, while the contribution rate of the Theil index from 2010 to 2017 to the overall Theil

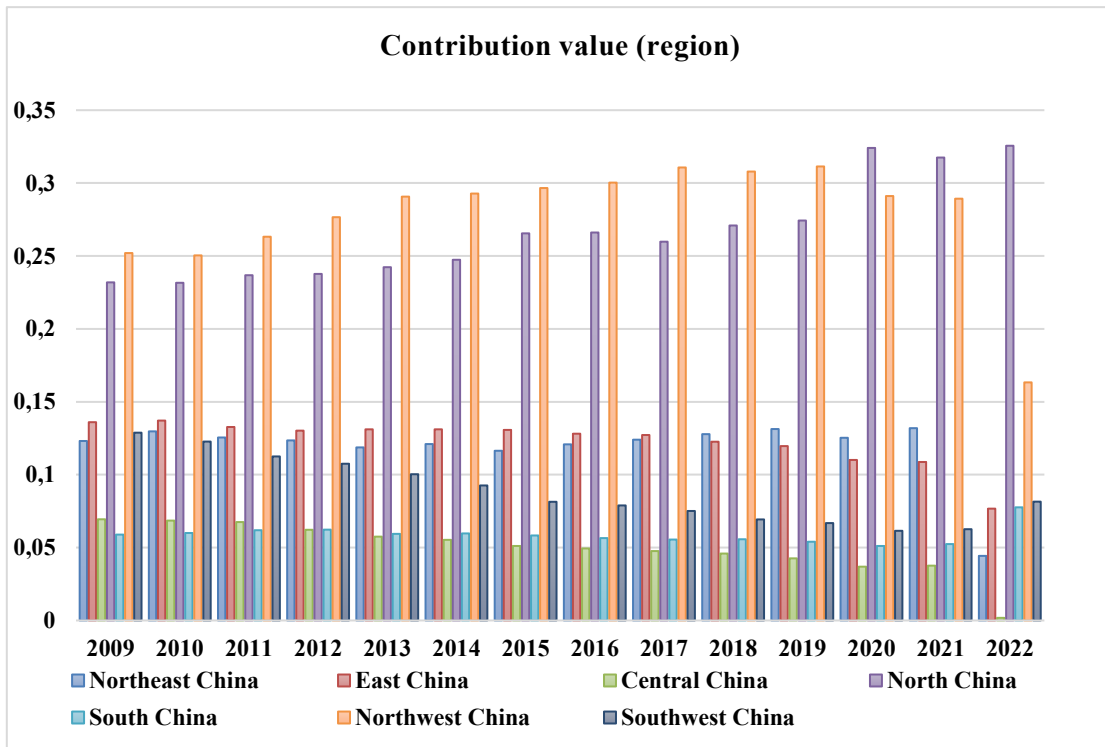
294

295 index has been decreasing year by year. Between 2018 and 2019, the contribution rate of inter-regional carbon  
 296 emissions has surpassed that within regions. According to the actual mean value of the Theil index contribution  
 297 regarding the inter-provincial carbon emission differences from 2010 to 2022, it can be deduced that: North  
 298 China>Northwest>Southwest>East China>South China>Northeast>Central China.

299 Table 3: Theil contribution values of carbon emissions by region from 2009 to 2022

Year	Northeast	East China	Central China	North China	South China	Northwest	Southwest
2009	0.0018	0.0398	0.0081	0.1892	0.0571	0.0488	0.0887
2010	0.0042	0.0410	0.0104	0.1799	0.0433	0.0568	0.0839
2011	0.0034	0.0373	0.0125	0.2035	0.0469	0.0805	0.0903
2012	0.0055	0.0439	0.0103	0.2109	0.0486	0.0766	0.0948
2013	0.0061	0.0384	0.0157	0.2179	0.0395	0.0808	0.1029
2014	0.0066	0.0476	0.0189	0.2323	0.0452	0.0881	0.0826
2015	0.0128	0.0583	0.0170	0.2597	0.0550	0.1039	0.0960
2016	0.0167	0.0721	0.0154	0.2778	0.0480	0.0964	0.1025
2017	0.0183	0.0778	0.0117	0.2736	0.0423	0.1263	0.0951
2018	0.0167	0.0810	0.0091	0.2837	0.0445	0.1542	0.0753
2019	0.0199	0.0819	0.0042	0.2996	0.0484	0.1693	0.0722
2020	0.0340	0.0789	0.0036	0.3090	0.0634	0.1688	0.0799
2021	0.0474	0.0778	0.0024	0.2864	0.0730	0.1659	0.0824
2022	0.0443	0.0767	0.0018	0.3256	0.0776	0.1633	0.0815

300  
 301 As shown in Figure 7, the mean value of Thiel contribution is 0.170 in Northeast China, 0.609 in East  
 302 China, 0.1011 in Central China, 0.2535 in North China, 0.0523 in South China, 0.1128 in Northwest China,  
 303 and 0.0877 in Southwest China. North China tops the values, with Central China at the bottom. This indicates  
 304 significant disparities in carbon emissions among regions, with pronounced differences within provinces. In  
 305 addition, according to the contribution rate index, East China is the highest, all above 70%; South China is the  
 306 lowest, less than 10%.



307

308

Figure 7 Theil contribution values for carbon emissions across regions in China - Bar Chart

309

Figure 8 further demonstrates the distribution of Theil contribution values of different provinces, plotting

310

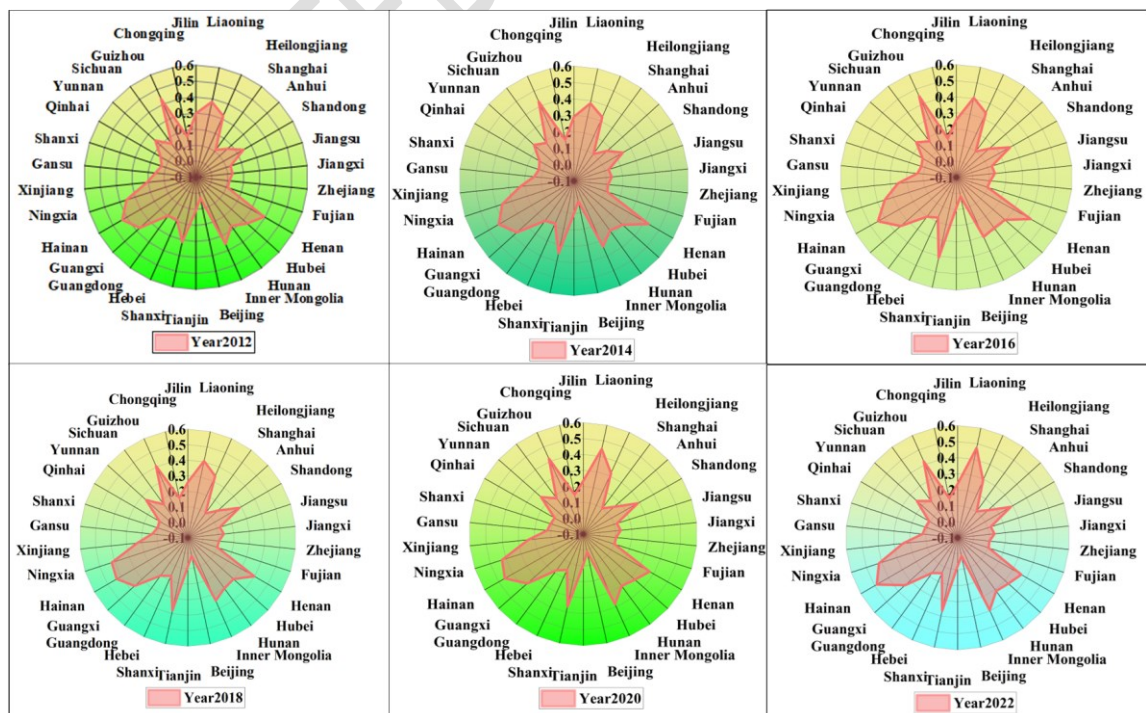
the distributions in 2012, 2014, 2016, 2018, 2020 and 2022. From the results, the Thiel index shows certain

311

changes in different years, especially the farther away from the year, the more significant the change. This test

312

further verifies the typical characteristics of spatial heterogeneity of China's carbon emissions.



313

Figure 8 Map of Theil contribution value of carbon emissions in different provinces (2012-2022)

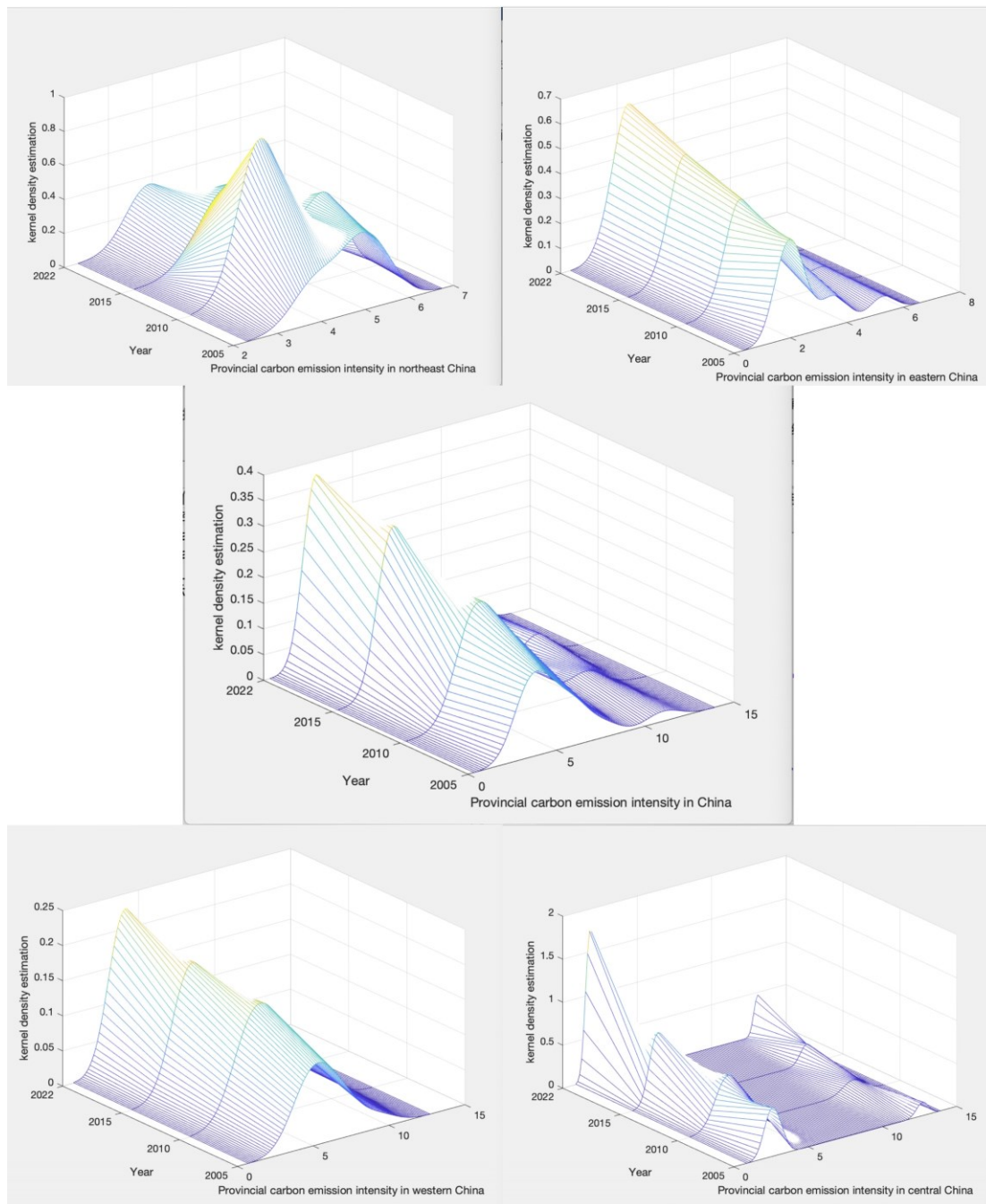
---

### 314 4.3 Discussion of carbon emission intensity results based on kernel density estimation model

315 The distribution curve of kernel density estimation is plotted as shown in Figure 8 to further compare the  
316 carbon emission characteristics of different regions.

317 As shown in Figure 8, considering the position of the curves, the centers of the kernel density functions for  
318 the three regions excluding the Northeast, as well as the national trend, have shown a tendency to move to the  
319 left and then to the right between 2005 and 2021. In the Northeast region, the peak shifted from a bimodal to a  
320 unimodal pattern between 2005 and 2010, indicating a reduction in polarization. Among them, the changes in  
321 the western region were more pronounced. In contrast, the changes in the whole country and the eastern region  
322 were relatively small, indicating that the magnitude of changes in carbon emission intensity across various  
323 regions was inconsistent. Furthermore, the kernel density tends to move towards lower values.

324 From the peak change of the curve, the peak density of all regions showed a decline from 2005 to 2015.  
325 The shape of the density function curve in the eastern, western and central regions and the whole country shifted  
326 from a sharp peak to a broader peak, while the Northeast region exhibited a trend of narrowing from a broad to  
327 a sharp peak. This indicates that the carbon emission intensity in different regions presents U-shaped and inverted  
328 U-shaped changes. Finally, upon examining the results from 2016 to 2022, the variations in the curves across  
329 different regions have narrowed, showing dynamic convergence. Possible reasons: With the concept of green  
330 development, the Chinese government has introduced a series of policies to reduce carbon emissions, effectively  
331 suppressing the growth of carbon emission intensity.



332

333

334

Figure 8: Distribution Curves of Carbon Emission Kernel Density Estimation in Different Regions

### 335 5. Conclusion

336

337

338

339

340

Based on the typical fact that "reducing carbon emissions" can promote the low-carbon circular development of the economy and society, this article uses panel data from 2005 to 2022 to analyze the impact of carbon emission reduction on China's economic growth, industrial structure, and energy consumption. This article systematically analyzes the carbon emission intensity of provinces in China, thoroughly examining the intensity characteristics, regional spatial disparities, and the trends of spatiotemporal evolution. The principal

---

341 research findings are as follows:

342 First, from a holistic perspective, the distribution of carbon emission intensity in China is characterized by  
343 significant regional heterogeneity, with significant differences in emissions among regions. The distribution of  
344 the centroid of the geometric ellipse of China varies from  $[[110^{\circ}0' \sim 110^{\circ}43'] E, [35^{\circ}52' \sim 37^{\circ}23'] N$ , indicating  
345 that the carbon emission intensity in eastern and southern China is higher than that in western and northern China.

346 Secondly, resulting from technological progress and economic growth during the sample period, the overall  
347 difference in China's carbon emission intensity decreased yearly but showed a "U" shaped fluctuation trend. In  
348 terms of carbon emission intensity, the carbon intensity of the eastern region rebounded to 1.41 billion tons per  
349 billion yuan in 2021 and dropped back to 1.27 billion tons per billion yuan in 2022. In 2019, the figure for central  
350 region dropped to 1.12 billion tons/billion yuan, rebounded to 1.35 billion tons/billion yuan in 2021, and dropped  
351 back to 1.21 billion yuan in 2022. In 2019, the carbon intensity of the western region fell to 3.08 billion  
352 tons/billion yuan, and rebounded to 3.36 billion tons/billion yuan in 2021. The carbon intensity of the Northeast  
353 region in 2019 was 810 million tons/billion yuan, and it rebounded to 990 million tons/billion yuan in 2022,  
354 making the Northeast region the area with the lowest carbon intensity.

355 Thirdly, according to the test results, regional differences have a significant impact on carbon emissions.  
356 The Theil index decomposition results reveal that inter-regional carbon emission disparities were less  
357 pronounced than intra-regional differences from 2010 to 2017, yet exceeded them from 2018 to 2022. This trend  
358 highlights the necessity for provinces to harness the carbon trading market's potential in reducing carbon  
359 emissions.

360 Fourthly, from the perspective of the national spatial pattern of provincial carbon emissions, the spatial  
361 distribution of provincial carbon emissions in China shows a trend of "high in the east and low in the west, dense  
362 in the north and sparse in the south". From 2005 to 2015, the kernel density curve showed a downward trend in  
363 general, with the centers of carbon emission kernel density functions in various regions showing distinct patterns  
364 of convergence. The spatial evolution of carbon emission intensity in different regions during 2016-2022 showed  
365 a decreasing trend, indicative of dynamic convergence. At the same time, according to the two-dimensional and  
366 three-dimensional curves of the kernel function, it is found that the carbon emission distribution in different  
367 regions generally presents a trend from agglomeration to dispersion. However, in 2022, the national and western  
368 regions experienced a weakening in their concentration trends; the spatial disparity in carbon intensity within the  
369 central region gradually diminished; and the Northeast region saw a transition from a bimodal to a unimodal  
370 peak in its curve, indicating a decline in polarization.

---

371 The above conclusions hold important theoretical and practical value. At the existing policy level, it is  
372 necessary to combine the carbon emission differences and economic development status of different regions,  
373 give priority to the implementation of carbon trading system for eastern provinces and cities with large carbon  
374 emissions and economically developed enterprises, and promote the green economic transformation. Moreover,  
375 it is crucial for the national government to set reasonable emission reduction targets for all provinces and cities,  
376 and allocate carbon emission quotas for different regions according to the development status of different  
377 provinces and cities. To establish a complete unified carbon trading market, it is also necessary to consider the  
378 carbon intensity of neighboring provinces, establish a sound regional carbon emission reduction cooperation  
379 mechanism, and advance the green development of provinces in accordance with local conditions.

380 **Ethics approval and consent to participate**

381 Not applicable.

382 **Consent for publication**

383 Not applicable.

384 **Availability of data and materials**

385 Not applicable.

386 **Competing interests**

387 The authors have no conflicts of interest to declare.

388 **Funding**

389 This research was funded by 2023 National Foreign Experts Project of the Ministry of Science and Technology  
390 of China (No. DL202320202L), by Tianjin art science planning general project (No. B24017), by China Civil  
391 Aviation High-quality Development Research Center 2023 open fund key project (No. ADI2023-1-02).

392 **Authors' contributions**

393 Gang Zeng, Yi Guo, Song Nie: Conceptualization, Investigation, Resources, Writing –original draft, review &  
394 editing. Keyan Liu, Yue Cao, Ling Chen, Dezhe Ren: Writing – original draft, Writing – review & editing. Jiaqi  
395 Zhang, Bowen Yan: Writing – review & editing.

396 **Acknowledgements**

397 Not applicable.

398 **Authors' information (optional)**

399 Not applicable.

400 **References**

401 Andrea F., Nastia D., Ivana M., et al., 2021. Greenhouse gas emissions reduction potential by using



---

402 antifouling coatings in a maritime transport industry. *Journal of Cleaner Production*, 2021: 295.

403 Andrea F., Nastia D., Ivana M., et al., 2022. Energy savings potential of hull cleaning in a shipping industry.

404 *Journal of Cleaner Production*, 2022: 374.

405 Chang Y.M., 2022. The logical approach, connotation, and practical application of promoting the "dual

406 carbon" work in the report of the 20th CPC National Congress. *Environment and Development*, 2022: 1-6+21.

407 Chen, J., Wang, H., Yin, W., et al., 2024. Deciphering carbon emissions in urban sewer networks: Bridging

408 urban sewer networks with city-wide environmental dynamics. *Water Research*, 2024: 121576.

409 Cheng Y., Zhang Y., Wang J.J., 2023. China Provincial Carbon Emissions Research on the Spatiotemporal

410 Evolution of Performance and Technology Innovation Driving. *Geographical Science*, 2023: 313-323.

411 Cui R., Li G.F., 2021. Regional disparities and dynamic evolution of China's Internet development level:

412 2006-2018. *Journal of Quantitative Economics and Technology Economics*, 2021: 3-20.

413 Cui, Y., Su, W., Xing, Y., Hao, L., Sun, Y., Cai, Y., 2023. Experimental and simulation evaluation of

414 CO<sub>2</sub>/CO separation under different component ratios in blast furnace gas on zeolites. *Chemical Engineering*

415 *Journal*, 2023:144579.

416 Dai X.W., He Y.Q., Zhong Q.B., 2015. Analysis of driving factors of China's agricultural carbon emissions

417 based on the extended Kaya identity. *Journal of University of Chinese Academy of Sciences*, 2015: 751-759.

418 Du H.B., Zhao L.J., Liu C.W., et al. 2022. Urban Areas Based on LEAP Model and KAYA Model Carbon

419 peak prediction and uncertainty analysis. *Journal of Ecology and Rural Environment*, 2022: 983-991.

420 Dussaux D., Vona F., Antoine D., 2023. Imported carbon emissions: Evidence from French manufacturing

421 companies. *Canadian Journal of Economics/Revue canadienne d'économique*, 2023: 593-621.

422 Guo P., Liang D., 2022. Does the low-carbon pilot policy improve the efficiency of urban carbon emissions:

423 Quasi-natural experimental research based on low-carbon pilot cities. *Journal of Natural Resources*, 2022: 1876-

424 1892.

425 Hai C.X., Yan L.L., Ying J.Z., et al., 2022. Analysis of spatial associations in the energy-carbon emission

426 efficiency of the transportation industry and its influencing factors: Evidence from China. *Environmental Impact*

427 *Assessment Review*, 2022: 97.

428 Hao Y.W., Han J.H., Wen K.C., et al., 2022. Estimation and spatiotemporal analysis of the carbon-emission

429 efficiency of crop production in China. *Journal of Cleaner Production*, 2022: 371.

430 Jian H., Lin C., Na Z., 2022. A Statistical Review of Considerations on the Implementation Path of China's

431 "Double Carbon" Goal. *Sustainability*, 2022: 11274-11274.

432 Jin P.L., De L.W., 2022. Analysis on the dynamic evolution of the equilibrium point of carbon emission

433 penetration for energy-intensive industries in China: based on a factor-driven perspective. *Environmental science*

434 *and pollution research international*, 2022: 5178-5196.

435 Kamani, H., Baniasadi, M., Abdipour, H., Mohammadi, L., Rayegannakhost, S., Moein, H., & Azari, A.,

436 2023. Health risk assessment of BTEX compounds (benzene, toluene, ethylbenzene and xylene) in different

---

437 indoor air using Monte Carlo simulation in zahedan city, Iran. *Heliyon*, 2023

438 L C.B., L S.S., S E.E., et al., 2021. Ambient PM<sub>2.5</sub>/sub Organic and Elemental Carbon in New York  
439 City: Changing Source Contributions During a Decade of Large Emission Reductions. *Journal of the Air Waste*  
440 *Management Association*, 2021: 995-1012.

441 Lee J., Lumley D., Lim U.Y., 2022. Improving total organic carbon estimation for unconventional shale  
442 reservoirs using Shapley value regression and deep machine learning methods. *AAPG Bulletin*, 2022.

443 Li L., Zhang B., Xia Q.Y., et al., 2023. The spatial effect of mismatched carbon emission efficiency of land  
444 resources and its impact path: empirical evidence from 108 cities in the Yangtze River Economic Belt. *Resources*  
445 *Science*, 2023: 1059-1073.

446 Li Z., Yang Y., So N., et al., 2023. Carbon footprint of maize planting under intensive subsistence cultivation  
447 in South Korea. *International Journal of Climate Change Strategies and Management*, 2023: 301-321.

448 Li, B., Wang, J., Nassani, A. A., et al., 2023. The future of Green energy: A panel study on the role of  
449 renewable resources in the transition to a Green economy. *Energy Economics*, 2023: 107026.

450 Liu H.J., Wang Y.H., Lei M.Y., 2019. Spatial Agglomeration and Evolution of China's Strategic Emerging  
451 Industries. *Journal of Quantitative Economics and Technology Economics*, 2019: 99-116.

452 Liu, X., Zhu, C., Kong, M., et al., 2024. The Value of Political Connections of Developers in Residential  
453 Land Leasing: Case of Chengdu, China. *Sage Open*, 2024.

454 Liu, X., Zhu, C., Kong, M., Yin, L., & Zheng, W., 2024. The Value of Political Connections of Developers  
455 in Residential Land Leasing: Case of Chengdu, China. *Sage Open*, 2024.

456 Liu, Z., Xu, Z., Zhu, X., et al., 2024. Calculation of carbon emissions in wastewater treatment and its  
457 neutralization measures: A review. *Science of The Total Environment*, 2024: 169356.

458 Liu, Z., Zhao, Y., Wang, Q., et al., 2024. Modeling and Assessment of Carbon Emissions in Additive-  
459 Subtractive Integrated Hybrid Manufacturing Based on Energy and Material Analysis. *International Journal of*  
460 *Precision Engineering and Manufacturing-Green Technology*, 2024.

461 Luo X., Ao X., Zhang Z., et al., 2020. Spatiotemporal variations of cultivated land use efficiency in the  
462 Yangtze River Economic Belt based on carbon emission constraints. *Journal of Geographical Sciences*, 2020:  
463 535-552.

464 Luo, J., Zhuo, W., Liu, S., et al., 2024. The Optimization of Carbon Emission Prediction in Low Carbon  
465 Energy Economy Under Big Data. *IEEE Access*, 2023:14690-14702.

466 Lv Y., Chen Z.Q., 2016. Research on Energy Consumption, Nitrogen Emissions and Their Influencing  
467 Factors in Zhejiang Province Based on Kaya Expansion. *Journal of Zhejiang University: Science Edition*, 2016:  
468 610-615+624.

469 Meng L.X., Yang C.H., Li H.B., et al., 2018. Analysis of regional differences in water pollutant emission  
470 intensity in China based on Theil index. *Environmental Pollution and Control*, 2018: 241-246.

471 Mohammad Z., Mehdi P., Ali M.F., et al., 2021. A highly carbon - efficient and techno - economically

---

472 optimized process for the renewable - assisted synthesis of gas to liquid fuels, ammonia, and urea products.  
473 *International Journal of Energy Research*, 2021: 16362-16382.

474 Najul L., Nikhil K., Chandra P.B., et al., 2022. Carbon emission intensity and firm performance: An  
475 empirical investigation in Indian context. *Journal of Statistics and Management Systems*, 2022: 1073-1081.

476 Qiu, L., Yu, R., Hu, F., et al., 2023. How can China's medical manufacturing listed firms improve their  
477 technological innovation efficiency? An analysis based on a three-stage DEA model and corporate governance  
478 configurations. *Technological Forecasting and Social Change*, 2023: 122684.

479 Song L., Lv J., 2017. Measuring the Regional Differences in Environmental Regulation Intensity in China  
480 Based on Theil Index. *Shandong Social Sciences*, 2017: 140-144.

481 Sun, C., Chen, J., He, B., et al., 2024. Digitalization and carbon emission reduction technology R&D in a  
482 Stackelberg model. *Applied Economics Letters*, 2024: 1-6.

483 Tao F., Debin F., Bolin Y., 2022. Carbon emission efficiency of thermal power generation in China:  
484 Empirical evidence from the micro-perspective of power plants. *Energy Policy*, 2022: 165.

485 Wang H., Wang S.Q., 2015. Dynamic evolution and spatial spillover effect of China's industrial CO<sub>2</sub>  
486 emission performance. *China Population, Resources and Environment*, 2015: 29-36.

487 Wang S.B., Zhuang G.Y., Dou X.M., 2023. Province of China Domain carbon Peak-echelon division and  
488 differentiated emission path: an investigation based on the dual perspectives of carbon emissions and economic  
489 development. *Wuhan University (Philosophy and Social Sciences Edition)*, 2023: 136-150.

490 Wang Z.F., Huang D.C., 2023. Comparison of Carbon Emission Efficiency of Transportation in the Yangtze  
491 River Economic Belt and the Yellow River Basin and Its Influencing Factors. *China Population, Resources and  
492 Environment*, 2023: 1-15.

493 Wei S., Hengye D., 2022. Measurement of provincial carbon emission efficiency and analysis of  
494 influencing factors in China. *Environmental science and pollution research international*, 2022: 38292-38305.

495 Wei S., Hengye D., 2022. Measurement of provincial carbon emission efficiency and analysis of  
496 influencing factors in China. *Environmental science and pollution research international*, 2022: 38292-38305.

497 XZ., XZ., K L., 2022. Regional differences and dynamic evolution of China's agricultural carbon emission  
498 efficiency. *International Journal of Environmental Science and Technology*, 2022: 4307-4324.

499 Xiao H.L., Xiang Y.T., Yao W., et al., 2022. Improving carbon emission performance of thermal power  
500 plants in China: An environmental benchmark selection approach. *Computers Industrial Engineering*, 2022: 169.

501 Xu L.L., Shu L.C., Li W., et al., 2023. Spatial and temporal evolution characteristics of groundwater  
502 extraction in China from 2000 to 2020. *Water Resources Protection*, 2023: 79-85+93.

503 Xu, A., Song, M., Wu, Y., et al., 2024. Effects of new urbanization on China's carbon emissions: A quasi-  
504 natural experiment based on the improved PSM-DID model. *Technological Forecasting and Social Change*,  
505 2024: 123164.

506 Xu, H., Yang, C., Li, X., et al., 2024. How do fintech, digitalization, green technologies influence sustainable

---

507 environment in CIVETS nations? An evidence from CUP FM and CUP BC approaches. *Resources Policy*, 2023:  
508 104994.

509 Ya Y.Z., Rui Y.C., Peng Z., et al., 2021. Spatiotemporal patterns of global carbon intensities and their driving  
510 forces. *The Science of the total environment*, 2021: 818151690-151690.

511 Yu F.R., Wan R.Y., Bi T.Z., et al., 2022. Does improvement of environmental efficiency matter in reducing  
512 carbon emission intensity? Fresh evidence from 283 prefecture-level cities in China. *Journal of Cleaner  
513 Production*, 2022: 373.

514 Yuan X.I., Yang Y., Sheng X.R., et al., 2023. Carbon peak Analysis of the Neutralization Policy and  
515 countermeasures. *Journal of Shandong University (Engineering Edition)*, 2023: 132-141.

516 Zhang M.d., Xi S.J., 2023. Evaluation of carbon emission efficiency of resource-based cities and its policy  
517 enlightenment. *Journal of Natural Resources*, 2023: 220-237.

518 Zhang Y.Y., Chen F.Y., Xu X., et al. 2023. Analysis of carbon emission effects of land use in Fujian Province  
519 based on county scale. *Environmental Science Research*, 36, 1446-1456.

520 Zhang, R., Yin, L., Jia, J., et al., 2019. Application of ATS-GWIFBM Operator Based on Improved Time  
521 Entropy in Green Building Projects. *Advances in Civil Engineering*, 2019: 3519195.

522 Zhao F.W., Hai Q.S., 2023. Spatiotemporal differences in and influencing factors of urban carbon emission  
523 efficiency in China's Yangtze River Economic Belt. *Environmental science and pollution research international*.

524 Zhao G.M., Zhao G.Q., Chen L.Z., et al. 2017. Spatial and temporal evolution and transition mechanism of  
525 China's carbon emission intensity. *China Population, Resources and Environment*, 2023: 27, 84-93.

526 Zhao, S., Zhang, L., An, H., et al., 2023. Has China's low-carbon strategy pushed forward the digital  
527 transformation of manufacturing enterprises? Evidence from the low-carbon city pilot policy. *Environmental  
528 Impact Assessment Review*, 2023: 107184.

529 Zhao, S., Zhang, L., Peng, L., et al., 2024. Enterprise pollution reduction through digital transformation?  
530 Evidence from Chinese manufacturing enterprises. *Technology in Society*, 2024: 102520.

531 Zheng, C., Chen, H., 2023. Revisiting the linkage between financial inclusion and energy productivity:  
532 Technology implications for climate change. *Sustainable Energy Technologies and Assessments*, 2023 :  
533 103275.

534 Zheng, S., Hai, Q., Zhou, X., et al., 2024. A novel multi-generation system for sustainable power, heating,  
535 cooling, freshwater, and methane production: Thermodynamic, economic, and environmental analysis. *Energy*,  
536 2023:130084.

537 Zhou C.Y., Wang Z., Zheng Y., et al., 2023. A study on the spatial differentiation of carbon amounts in the  
538 county's "Collaborative Carbon Control Alliance" from the perspective of scaling reorganization—an analysis  
539 based on the carbon reduction potential of Zhejiang Province. *Geographic Research*, 2023: 1545-1559.